Please cite as: [Franciosa P., Palit A., Gerbino S., Ceglarek D., *A Novel Hybrid Shell Element Formulation (QUAD+ and TRIA+): A Benchmarking and Comparative Study*, Finite Elements in Analysis and Design, Volume 166, 15 November 2019, 103319]

A novel hybrid shell element formulation (QUAD+ and TRIA+): A benchmarking and comparative study

Pasquale Franciosa[a], Arnab Palit[a], Salvatore Gerbino[b], Darek Ceglarek[a]

[a] Digital Lifecycle Management (DLM), WMG, University of Warwick, CV47AL, Coventry, UK

[b] DiBT - Engineering Division, University of Molise, Via De Sanctis, 86100 Campobasso, IT

Corresponding Author:

Arnab Palit
Digital Lifecycle Management (DLM),
WMG, University of Warwick,
Coventry, UK
CV4 7AL
Email: a.palit.1@warwick.ac.uk; arnabpalit@gmail.com
Tel: +44 (0) 24 7657 72422

Please cite as: [Franciosa P., Palit A., Gerbino S., Ceglarek D., *A Novel Hybrid Shell Element Formulation (QUAD+ and TRIA+): A Benchmarking and Comparative Study*, Finite Elements in Analysis and Design, Volume 166, 15 November 2019, 103319]

Abstract:

This paper introduces a novel hybrid finite element (FE) formulation of shell element to enable assembly process simulation of compliant sheet-metal parts with higher efficiency and flexibility. Efficiency was achieved by developing both new hybrid quadrilateral and triangular elements. Quadrilateral element (QUAD+) was formulated by combining area geometric quadrilateral 6 (AGQ6) nodes and mixed interpolated tensorial components (MITC) to model membrane and bending/shear component respectively. Triangular element (TRIA+) was formulated by merging assumed natural deviatoric strain (ANDES) for membrane and MITC for bending/ shear component. Flexibility was addressed by developing an open-source C++ code, enhanced by the OpenMP interface for multiprocessing programming. Tests and benchmarks were compiled and executed within Matlab using the MEX API interface. Extensive benchmark studies were accomplished to evaluate the performance of the proposed hybrid formulation and the shell formulations used in three FEM packages - ABAQUS, ANSYS and COMSOL- under static linear elastic condition with small strain assumption. It was observed that the proposed QUAD+ and TRIA+ elements performed better amongst the FE packages, especially when there was in-plane mesh distortion, with errors below 3%. It was also identified that the best efficiency is obtained by adopting dominant QUAD+ elements compared to the TRIA+ when working on complex geometries. This paper also contributes to present a wide set of benchmark studies required to verify new release of FE packages using shell element or evaluate the performance of new shell formulations.

Keywords: Finite element modelling, shell elements, benchmark study, sheet metal, flexibility and efficiency

1. Introduction:

Advancement in numerical methods and simulation techniques enable engineers to solve PDE's in a wide range of engineering disciplines such as structural and solid mechanics, heat transfer, fluid dynamics, electromagnetics and many other areas. During the past several decades, finite element method (FEM) is the most adopted numerical technique to solve PDEs, although other method exits such as boundary element method (BEM) [1] or mesh less method [2] etc. One of the dominant area of FEM application is involved with the analysis of shell structure to estimate part deformation, and residual stress due to assembly process of compliant sheet parts in the manufacturing, automobile, aeronautical, civil and biomedical industries [3-6]. Many successful commercial FEM-based packages are available to perform shell element modelling to a wide range of engineering analyses. ANSYS, ABAQUS, COMSOL are the most popular amongst them for academics and industrial professionals. Besides, a number of home-made simulation tools can also be found in literature or on the web that are developed to solve very specific problems using shell element modelling by losing in generality but offering the expected level of customisation within a particular design context.

Three main aspects should be considered while selecting a FEM based simulation tool for shell element modelling: (a) accuracy, (b) efficiency, and (b) flexibility [7-10]. Although accuracy is utmost important for FE analysis, computational time required to solve a real life engineering problem using FEM is also a crucial factor. A more critical scenario arises during design optimisation where thousands of simulations are usually required to explore the design space (e.g. during compliant sheet metal assembly simulation and optimisation). Engineers aim to get suitable and accurate results in reasonable time, which is sometimes not achievable due to the complexity of the problem even with powerful computational systems (HPC or cloud computing etc.). For example, an optimisation problem is solved by population based heuristics such as genetic algorithm (GA) where the fitness function is calculated using FEM. If each FEM simulation takes 1 min to solve, the population size in GA is 100, and the GA converges after 200 iterations, the total time to solve the optimisation would take more than (100*200*1) min i.e. 333.33 hrs or approximately 2 weeks. However, if the same FEM problem could have been solved using efficient formulation which takes 40 s to solve each FEM simulation, the total time would have been required to solve the problem would be (100*200*40) s i.e. 222.22 hrs or approximately 10 days. Therefore, efficiency of the shell element modelling is a critical factor in getting accurate results in reasonable time. It could be thought as the ratio between the level of accuracy and the mesh complexity (or density/number). Higher efficiency leads to a very accurate results even with a coarse mesh, and subsequently, it reduces computational time. Theoretically, shell elements formulation should satisfy basic numerical tests (e.g. the isotropy, zero energy mode and patch tests) and depicts good convergence for different type of shell behaviours problems such as membrane dominated, bending dominated and combined behaviours irrespective of geometry, boundary and loading conditions, and shell mesh configurations used in the problem [5]. In this paper, a novel hybrid formulation, that is a combination of two different formulations, was used for bending and membrane components of shell element modelling for improving the efficiency of the FE computation with the application in compliant sheet metal assembly simulation. It was termed 'hybrid' as the formulation was developed by combining two different but well-known formulations that worked in a different way but would provide better results if combined. Quadrilateral element (QUAD+) was formulated by combining area geometric quadrilateral 6 (AGQ6) [11] nodes and mixed interpolated tensorial components (MITC) [12, 13] to model membrane and bending/shear component respectively. Triangular element (TRIA+) was formulated by merging assumed natural deviatoric strain (ANDES) [14-17] for membrane and MITC for bending/shear component.

On the other hand, flexibility measures the ease of customisation of the simulation tool to include specific new features depending on the process being simulated [18, 19]. Although, ANSYS, ABAQUS, COMSOL are the most popular software used by academics and industrial professionals, this commercial software often does not permit an easy integration with other simulation or designing

software through high level programming languages, and therefore, the flexibility is not very high. Usually, customisation is made by defining sub-routines, (often called UDF - User Defined Function) written in some programming languages, which is cumbersome for the researchers. In addition, the multidisciplinary nature of the complex engineering problems often involves non-linear conditions with uncertainties which impede the reliability of the FEM predictions. In such scenarios, the use of other advanced techniques such as response surface method, machine learning, curve fitting, model-based calibration, neural networks, evolutionary optimization, inverse approaches, or hybrid experimental-numerical techniques might compensate the uncertainties, yielding results that are otherwise unattainable only through FEM simulation [3]. Therefore, it is paramount that the simulation model of compliant sheet metal assembly must have the capability of integrating FEM modelling with other aspects of assembly modelling such as stochastic variation, machine learning, curve-fitting, optimisation etc. In this context, Matlab is an effective tool to develop powerful FEM simulation routines based on FEM by using its high level programming language and its capabilities to model other advance engineering techniques, and to combine them with each other [20].

As aforementioned, developing an accurate and efficient tool for shell element modelling, which at the same time offers a certain level of flexibility for ease of customisation, is a challenging task to be achieved. In this paper, hybrid formulation (QUAD+ and TRIA+) of shell element was proposed, and an in-house Matlab-based tool was developed to address this challenge i.e. improve accuracy, efficiency and flexibility for compliant sheet metal assembly application. The computationally expensive part of the modelling was implemented in C++ using Mex interface. Parallel computing was employed using OpenMp platform in C++ [21]. The flexibility is increased as the model could easily be combined with robot kinematics programming, stochastic part-variation modelling, machine learning, optimisation techniques or many other aspects of an assembly simulation using high level programming language in Matlab. Therefore, the developed in-house tool includes both higher flexibility (ease of integration) and higher efficiency (to provide accurate results even with a coarse mesh) which are the cornerstone of selecting any simulation toolbox. A wide set of benchmark problem was carried out to explore the effect of newly developed hybrid shell element formulation (hereafter called QUAD+ and TRIA+). In addition, a comparative study was performed to evaluate the performances of proposed hybrid formulation (QUAD+ and TRIA+) and the shell element formulation used in three commercial FEM packages (ABAQUS, ANSYS and COMSOL). These Benchmarks tests were selected to highlight the sensitivity of numerical results on mesh distortion, and on membrane and shear locking phenomena, which might affect the efficiency of shell elements. Therefore, the key aspects of the paper are as follows:

(a) To provide a brief overview of the developed hybrid shell element formulation to achieve high efficiency with accurate and robust outcomes.
(b) To evaluate the performances of shell element formulation used in three commercial FEM packages (ABAQUS, ANSYS and COMSOL) and the proposed hybrid shell element (QUAD+ and TRIA+) formulation under static linear elastic condition with small strain deformation.
(c) To provide a condensed documentation of required benchmark studies to verify a new release of a simulation package using shell element or evaluate the performances of a new shell formulation under static liner elastic condition.

The paper is arranged as follows: Section 2 provides a brief overview of the proposed hybrid shell element formulation along with a brief review of the shell elements used in ABQUAS, ANSYS and COMSOL; Section 3 presents the benchmark tests and the related results; finally, Section 4 and 5 draw discussion and final remarks.

2. Background of Shell element formulation

A shell element should be applicable to simple plate geometries as well as complex shell geometries for both thick and thin structures, i.e. door or bonnet assembly in automotive applications. Moreover, shell element should provide good accuracy for at least displacement calculation with relatively low computational time. Lastly, it should present low sensitivity to mesh distortion.

The discrete Kirchoff element, combined with membrane capability, may be considered one of the most suitable elements for shell modelling. However, this element does not consider the effect of shear deformation, and therefore, it is valid only for thin geometry [13]. On the contrary, the Reissner-Mindlin formulation accounts for shear deformation by decoupling the rotation of plate cross-section from the slope of the deformed mid-surface [12, 13]. The main drawback of this parametric displacement-based model is that a shear locking phenomenon will occur when the plate becomes thinner [13]. To overcome this shortcoming, three main approaches were embraced in the literature: (a) reduced/selective integration [10], (b) mixed interpolation for both generalised displacements (translations and rotations) and transverse shear strains [13, 22], and (c) non-conforming element method [23, 24]. As reported in some comparison studies [12, 25], the mixed interpolation approach (also called MITC - Mixed Interpolated Tensorial Components) provides satisfactory and stable results. Therefore, MITC formulation was preferred as a base model for this work. On the other hand, the objective of the work was to use linear shell element formulation (1st order polynomial) and tried to avoid any higher order shell element formulations as a base model for hybrid formulation. This is due to the fact that the construction and application of higher order shell elements is somehow restricted for complex geometries with holes, edges, or complex boundary conditions, and there is always an additional numerical cost for creating these higher order element compared to h-refinement which is available in any standard software. Due to the aforementioned reasons, MITC4 and MITC3 formulation [12, 13] was used as base model for quadrilateral and triangular mesh element respectively. For isotropic material, the shell element can be separated into a membrane element (in-plane) and a plate bending (out-of-plane) element [13]. In this paper, two different formulations were used to model membrane and bending/shear components respectively, and thereafter, the formulations were combined together to model the shell element. MITC4 and MITC3 formulation was used as base model for quadrilateral and triangular mesh element respectively for plate bending/shear component. On the other hand, AGQ6 [11] and ANDES [14-17] were selected for quadrilateral and triangular mesh element respectively for modelling membrane component as these formulations were shown insensitiveness in mesh distortion. Although shell elements can be successfully employed in a wide range of applications, such as non-linear dynamic analysis, heat transfer, fluid dynamic flows or complex coupled multi-physics, the in-house code was designed and developed to simulate assembly processes of sheet-metal parts under the assumption of static loads and boundary conditions with linear elastic small deformation.

A brief overview of these formulations, used for TRIA (triangular) and QUAD (quadrilateral) shell elements, are described in the following subsections. In this paper, the triplets (u_i, v_i, w_i) and (α_i, β_i, γ_i) (with respect to the i-th node) describe the translational and rotational DoFs along and around x, y and z axes, respectively. Table 1 shows the adopted quadrilateral (QUAD) and triangular (TRIA) shell elements for each tested software.

Table 1: Shell elements tested

Software	QUAD Elements	TRIA Elements
ABAQUS	S4	S3
ANSYS	SHELL63	SHELL63
COMSOL	MITC4	MITC3
In-house Matlab tool	QUAD+ (AGQ6-MITC)	TRIA+ (ANDES-MITC)

While for flat shell elements, the in-plane and the out-of-plane behaviours are completely decoupled, they become dependent for not-planar elements. This issue is called warping effect. It is particularly sensitive for QUAD elements where the nodes of the element are not located on a same plane (this usually happens for double-curved surfaces).

2.1 TRIA+ shell element formulation

The proposed hybrid TRIA+ shell element is a three-node element and adopts the MITC formulation for the bending behaviour and the ANDES (Assumed Natural DEviatoric Strain) template for the membrane part. Warping correction is not required since a triangular linear element is always planar.

2.1.1 TRIA+ element: Membrane component

The classical isoparametric membrane formulation of a three-node TRIA element only accounts two DoFs per node (for instance, in-plane translations u_i and v_i). It leads to a Constant Strain Triangle (CST). Hence, the CST formulation has no rotational stiffness for the drilling DoF (γ_i). To avoid the numerical instability due to zero-drilling stiffness, one common workaround is the introduction of a fictitious stiffness around the drilling direction (typically equal to 10^{-4} of the smallest K element along the diagonal). However, it was overserved through experiments that the drilling stiffness is problem dependent, and therefore, such a constant correction is not suitable for a general-purpose software. Therefore, the membrane component was implemented based on the assumed natural deviatoric strain (ANDES) formulation [14-17] to overcome the "manual" drilling stiffness correction. Basically, the ANDES allows to combine together the in-plane DoFs (u_i and v_i) and the drilling DoF (γ_i) by splitting the stiffness matrix into two contributions, as stated in Eq (1), where K_b is the 9x9 basic stiffness matrix (taking care of consistency), while K_h is the 9x9 higher order stiffness (taking care of numerical stability).

$$K_m = K_b + K_h \tag{1}$$

Alvin, et al. [26] proved that the K_b matrix can be obtained in a closed form as in Eq (2) where V is the volume of the element and D is the 3x3 elasticity matrix for plane stress condition.

$$K_b = \frac{1}{V} L \cdot D \cdot L^T \tag{2}$$

L is a 9x3 matrix, defined in equation (3), where *th* is the element thickness. x_{ij} and y_{ij} are the differences in node coordinates ($x_{ij}=x_i - x_j$; $y_{ij}=y_i - y_j$).

$$L=\frac{th}{2}\begin{bmatrix} y_{23} & 0 & x_{32} \\ 0 & x_{32} & y_{23} \\ \frac{1}{4}y_{23}\left(y_{13}-y_{21}\right) & \frac{1}{4}x_{32}\left(x_{31}-x_{12}\right) & \frac{1}{2}\left(x_{31}y_{13}-x_{12}y_{21}\right) \\ y_{31} & 0 & x_{31} \\ 0 & x_{13} & y_{31} \\ \frac{1}{4}y_{31}\left(y_{21}-y_{32}\right) & \frac{1}{4}x_{13}\left(x_{12}-x_{23}\right) & \frac{1}{2}\left(x_{12}y_{21}-x_{23}y_{32}\right) \\ x_{12} & 0 & x_{21} \\ 0 & x_{21} & y_{12} \\ \frac{1}{4}y_{12}\left(y_{32}-y_{13}\right) & \frac{1}{4}x_{21}\left(x_{23}-x_{31}\right) & \frac{1}{2}\left(x_{23}y_{32}-x_{31}y_{13}\right) \end{bmatrix} \tag{3}$$

Even the higher order stiffness (K_h) can be defined in a closed form (Eq. 4) so that the numerical integration is not required.

$$K_h = T_{\theta u}^T \cdot K_\theta \cdot T_{\theta u} \tag{4}$$

with

$$T_{\theta u}=\frac{1}{4A}\begin{bmatrix} x_{32} & y_{32} & 4A & x_{13} & y_{13} & 0 & x_{21} & y_{21} & 0 \\ x_{32} & y_{32} & 0 & x_{13} & y_{13} & 4A & x_{21} & y_{21} & 0 \\ x_{32} & y_{32} & 0 & x_{13} & y_{13} & 0 & x_{21} & y_{21} & 4A \end{bmatrix} \tag{5}$$

and

$$K_\theta = \frac{3}{4}\rho_0 \cdot th \cdot A\left(Q_4^T \cdot D_n \cdot Q_4^T + Q_5^T \cdot D_n \cdot Q_5 + Q_6^T \cdot D_n \cdot Q_6\right) \tag{6}$$

where,

$$\rho_0 = 0.5\left(1-4\cdot\nu^2\right) \tag{7}$$

$$D_n = T_e^T \cdot D \cdot T_e \tag{8}$$

$$Q_4=\frac{1}{2}\left(Q_1+Q_2\right),\quad Q_5=\frac{1}{2}\left(Q_2+Q_3\right),\quad Q_6=\frac{1}{2}\left(Q_1+Q_3\right) \tag{9}$$

$$Q_1=\frac{2A}{3}\begin{bmatrix} \frac{1}{L_{12}^2} & \frac{2}{L_{12}^2} & \frac{1}{L_{12}^2} \\ 0 & \frac{1}{L_{23}^2} & -\frac{1}{L_3^2} \\ -\frac{1}{L_{13}^2} & -\frac{1}{L_{13}^2} & -\frac{2}{L_{13}^2} \end{bmatrix}, Q_2=\frac{2A}{3}\begin{bmatrix} -\frac{2}{L_{12}^2} & -\frac{1}{L_{12}^2} & -\frac{1}{L_{12}^2} \\ \frac{1}{L_{23}^2} & \frac{1}{L_{23}^2} & \frac{2}{L_3^2} \\ -\frac{1}{L_{13}^2} & 0 & \frac{1}{L_{13}^2} \end{bmatrix}, Q_3=\frac{2A}{3}\begin{bmatrix} \frac{1}{L_{12}^2} & -\frac{1}{L_{12}^2} & \frac{0}{L_{12}^2} \\ -\frac{1}{L_{23}^2} & -\frac{2}{L_{23}^2} & -\frac{1}{L_3^2} \\ \frac{2}{L_{13}^2} & \frac{1}{L_{13}^2} & \frac{1}{L_{13}^2} \end{bmatrix} \tag{10}$$

$$T_e = \frac{1}{4A^2}\begin{bmatrix} y_{23}y_{13}L_{12}^2 & y_{31}y_{21}L_{23}^2 & y_{12}y_{32}L_{13}^2 \\ x_{23}x_{13}L_{12}^2 & x_{31}x_{21}L_{23}^2 & x_{12}x_{32}L_{13}^2 \\ \left(y_{23}x_{31}+x_{32}y_{13}\right)L_{12}^2 & \left(y_{31}x_{12}+x_{13}y_{21}\right)L_{23}^2 & \left(y_{12}x_{23}+x_{21}y_{32}\right)L_{13}^2 \end{bmatrix} \quad (11)$$

where, A is the area of the element, ν is the Poisson's ratio, and L_{ij} is the length of edge linking (i, j) nodes. As shown, Eq. (5) to (11) are used to calculate K_h.

2.1.2 TRIA+ element: bending and shear component

The DoFs of the plate bending component are the out-of-plane translation (w_i), and the two rotations α_i and β_i. Following the Reisner-Mindlin formulation, the 9x9 stiffness matrix (K_p) can be expressed by combining the bending and the shear effects, as defined by Eq (12). D_s is the 2x2 elasticity matrix under shear deformation while λ is the shear correction factor equal to 5/6 as used in COMSOL [27].

$$K_p = \frac{th^3}{12}\int_A B_b^T \cdot D \cdot B_b dA + \lambda \cdot th \int_A B_s^T \cdot D_s \cdot B_s dA \quad (12)$$

B_b and B_s are strain-displacement matrix for the bending and shear part respectively. Following the isoparametric formulation, B_b contains the derivatives of the shape functions, Ni(ξ,η), where (ξ,η) are the natural coordinates [28]. It can be written:

$$B_b = \begin{bmatrix} B_{b1} & B_{b2} & B_{b3} \end{bmatrix}$$
$$B_{bi=}\begin{bmatrix} 0 & 0 & \frac{\partial N_i}{\partial x} \\ 0 & -\frac{\partial N_i}{\partial y} & 0 \\ 0 & -\frac{\partial N_i}{\partial x} & \frac{\partial N_i}{\partial y} \end{bmatrix} \quad (13)$$

Based on the MITC formulation, the shear components are interpolated first on the tying points (artificial nodes added on the middle of each element side) and then expressed in terms of nodal DoFs [29] as govern by the following equations (Eq. 14 to 17).

$$B_s = \Omega_{12} \cdot C_{J,T} \cdot T_{\xi\eta,T} \quad (14)$$

$$\Omega_{12} = \begin{bmatrix} sin(\varphi_2) & -sin(\varphi_1) \\ -cos(\varphi_2) & cos(\varphi_1) \end{bmatrix} \quad (15)$$

$$C_{J,T} = \begin{bmatrix} \frac{\sqrt{x_{13}^2+y_{13}^2}}{\left|J(\xi,\eta)\right|} & 0 \\ 0 & \frac{\sqrt{x_{21}^2+y_{21}^2}}{\left|J(\xi,\eta)\right|} \end{bmatrix} \quad (16)$$

$$T_{\xi\eta,T} = \begin{bmatrix} -1 & -\frac{y_{21}+y_{32}\xi}{2} & \frac{x_{21}+x_{32}\xi}{2} & 1 & -\frac{y_{21}+y_{13}\xi}{2} & \dots \\ -1 & \frac{y_{13}+y_{32}\eta}{2} & -\frac{x_{13}+x_{32}\eta}{2} & 0 & \frac{y_{13}\eta}{2} & \\ \dots & \frac{x_{21}+y_{13}\xi}{2} & 0 & -\frac{y_{21}\xi}{2} & \frac{x_{21}\xi}{2} & \\ & -\frac{x_{13}\eta}{2} & 1 & \frac{y_{13}+y_{21}\eta}{2} & -\frac{x_{13}+x_{21}\eta}{2} & \end{bmatrix} \quad (17)$$

where ϕ_1 and ϕ_2 are the angles between ξ and x axis, and η and x axis respectively. |J| is the Jacobian of the transformation from the natural space to the Cartesian reference.

Finally, the numerical integration of the stiffness matrix in Eq (12) can be obtained using a three-point Gauss scheme.

2.2 QUAD+ shell element formulation

The proposed hybrid QUAD+ shell element is a four-node element and implements the MITC formulation for the bending behaviour and the area coordinate formulation for the membrane component. The warping correction matrix is also employed to couple bending and membrane component for not-planar elements.

2.2.1 QUAD+ element: Membrane component

Although the isoparametric coordinate has been widely applied in the constructions of quadrilateral membrane elements, such approach is sensitive to mesh distortion (i.e., parallelogram or trapezoidal elements). As a result, membrane locking might arise during simulation. In fact, the Jacobian matrix becomes ill-conditioned for highly distorted elements, and therefore, the Cartesian reference (x, y) would be badly described in terms of natural coordinates (ξ, η). This leads to poor numerical accuracy.

Area Geometric Quadrilateral 6 nodes (AGQ6), mainly based on quadrilateral area coordinate [11], was implemented in VRM to discard the drawbacks associated with isoparametric formulation. AGQ6 uses four classical bi-linear shape functions which correspond to the four-corner nodes, and two additional nodes which correspond to two fictitious internal DoFs. After static condensation, the internal DoFs vanish so that the element stiffness matrix is still an 8x8 matrix, accounting only in-plane translations u_i and v_i as shown

$$K_m = K_{qq} - K_{\lambda q}^T \cdot K_{\lambda\lambda}^{-1} \cdot K_{\lambda q} \quad (18)$$

$$\begin{aligned} K_{qq} &= th\int_A B_q^T \cdot D \cdot B_q dA \\ K_{\lambda\lambda} &= th\int_A B_\lambda^T \cdot D \cdot B_\lambda dA \\ K_{\lambda q} &= th\int_A B_\lambda^T \cdot D \cdot B_q dA \end{aligned} \quad (19)$$

where B_q and B_λ are the derivatives of the classical shape functions and the additional shape modes, respectively. The detailed analytical derivation of AGQ6 formulation can be found in [11].

2.2.2 QUAD+ element: Bending and shear component

The bending and shear behaviour are captured through MICT formulation. Similarly to the TRIA element, the out-of-plane translation (w_i), and the two rotations α_i and β_i are considered here. The 12x12 stiffness matrix is obtained using the same expression stated into Eq (12). Here a 2x2 Gauss rule was

employed. Moreover, the bending part can be inherited from Eq (13) and re-written as in Eq (20), whereas the shear components [12] can be expressed by Eq (21).

$$B_b = \begin{bmatrix} B_{b1} & B_{b2} & B_{b3} & B_{b4} \end{bmatrix}$$
$$B_{bi=} \begin{bmatrix} 0 & 0 & \frac{\partial N_i}{\partial x} \\ 0 & -\frac{\partial N_i}{\partial y} & 0 \\ 0 & -\frac{\partial N_i}{\partial x} & \frac{\partial N_i}{\partial y} \end{bmatrix} \qquad \forall i = 1,2,3,4 \tag{20}$$

and

$$B_s = \Omega_{12} \cdot C_{J,T} \cdot T_{\xi\eta,T} \tag{21}$$

Where,

$$C_{J,Q} = \begin{bmatrix} \frac{\sqrt{\left(C_x + B_x\xi\right)^2 + \left(C_y + B_y\xi\right)^2}}{8\left|J\left(\xi,\eta\right)\right|} & 0 \\ 0 & \frac{\sqrt{\left(A_x + B_x\eta\right)^2 + \left(A_y + B_y\eta\right)^2}}{8\left|J\left(\xi,\eta\right)\right|} \end{bmatrix} \tag{22}$$

$$T_{\xi\eta,Q} = \begin{bmatrix} \frac{1}{2}(1+\eta) & -\frac{1}{4}(1+\eta)y_{12} & \frac{1}{4}(1+\eta)x_{12} & -\frac{1}{2}(1+\eta) & -\frac{1}{4}(1+\eta)y_{12} & \frac{1}{4}(1+\eta)x_{12} \\ \frac{1}{2}(1+\xi) & -\frac{1}{4}(1+\xi)y_{14} & \frac{1}{4}(1+\xi)x_{14} & \frac{1}{2}(1-\xi) & -\frac{1}{4}(1-\xi)y_{23} & \frac{1}{4}(1-\xi)x_{23} \\ -\frac{1}{2}(1-\eta) & -\frac{1}{4}(1-\eta)y_{43} & \frac{1}{4}(1-\eta)x_{43} & \frac{1}{2}(1-\eta) & -\frac{1}{4}(1-\eta)y_{43} & \frac{1}{4}(1-\eta)x_{43} \\ -\frac{1}{2}(1-\xi) & -\frac{1}{4}(1-\eta)y_{23} & \frac{1}{4}(1-\eta)x_{23} & -\frac{1}{2}(1+\eta) & -\frac{1}{4}(1+\eta)y_{14} & \frac{1}{4}(1+\eta)x_{14} \end{bmatrix} \tag{23}$$

2.2.3 QUAD+ element: Warping correction

The above formulation for QUAD+ element is only valid for flat quadrilateral elements. For curved and complex structures, it is often not trivial and sometime impossible to locate all nodes of a four-node shell element in one plane, and then the initial geometry of the element is warped.

Once calculating the stiffness matrix for the projected flat element [30], the warpage correction is applied to it. Basically, two main approaches are available to deal with warped elements: the rigid-link method [31] and the force/moment correction approach [32, 33]. In VRM, the method proposed in [32] was implemented. In order to compensate the out-of-plane rotation due to non-coplanarity of nodes, additional forces and moments are added, depending on the signed distance of i-th node from the projected flat element.

The warping correction compensates the drilling rotation (the additional moment around z axis balances the drilling rotation). However, when the warped element becomes planar, such a correction vanishes and the stiffness matrix is ill-conditioned. Therefore, an artificial drilling stiffness (equal to 10^{-4} times the smallest entry in the stiffness matrix) is always added.

2.3 ABAQUS shell element

Elements S4 and S3 belong to ABAQUS general-purpose element library as they are suitable for the analysis of both thick and thin shell structures [34]. Moreover, the finite-strain formulation allows them to predict good results even in case of large deformations.

Element S4 is a fully integrated four-node finite-membrane-strain shell element. Since the fully integration is used, the element does not undergo zero energy modes (spurious membrane or bending), and therefore, hourglass stabilization is not used. To avoid the shear locking phenomenon (arising in applications dominated by bending deformation and approaching zero thicknesses), a MITC scheme is implemented mainly based on the model proposed in [12]. S4 uses a standard displacement formulation for the element's bending stiffness and a modified membrane formulation with a drilling rotation control. In particular, the membrane formulation is governed by the equilibrium of a three-dimensional body in a state of plane stress, considering an enhancement to the rate of deformation tensor.

The three-node S3 element results from degenerating a four-node element into a three nodes shell.

2.4 ANSYS shell elements

SHELL63 [35] element is a 3D four-node shell element which is fully integrated with both bending and membrane capabilities [36]. The element has six degrees of freedom at each node and its formulation includes stress stiffening and large deflection capabilities. SHELL63 by default uses shape functions without shear deflection with extra shape functions (often called not-conforming or hierarchical functions in [37]). As the in-plane rotational (drilling) degree of freedom (DoF) has no stiffness associated with it, a small stiffness is added to prevent a numerical instability and shear-locking. This approach is derived in [38].

The three-node SHELL63 element is obtained by the degeneration of the quadrilateral shell into a triangle.

2.4 COMSOL shell elements

Shell elements in COMSOL refer to Mindlin-Reissner plate theory to consider transverse shear deformation. Such a formulation includes large deformation capabilities and can be used for thin and thick shells. Shells in COMSOL have an MITC formulation essentially derived from the theory presented in [13]. Both QUAD and TRIA elements have five DoFs per node. Therefore, in-plane drilling DoF is not considered in COMSOL [27].

3. Benchmark tests – description and results

A number of linear elastic tests for shell element accuracy was proposed over the years. In [39], McNeal and Harder presented a set of performance tests in which several factors affecting the shell accuracy were considered. Later on, NAFEMS (http://www.nafems.org/) published a set of benchmarks for performance evaluation [40]. These tests have particular merit since they allow to detect element locking and sensitivity to mesh distortion.

3.1 Basic numerical tests

Three basic numerical tests [41, 42] (the isotropy, zero energy mode and patch tests) were performed for QUAD+ and TRIA+ shell element.

The triangular as well as quad element behaviour should not depend on the sequence of node numbering i.e. element orientation [41, 42]. This is called isotropy property, and the numerical procedure of the test was given in [43]. Both QUAD+ and TRIA+ passed the isotropy test.

In the zero energy mode tests, the number of zero eigenvalues of the stiffness matrix of a single unsupported element should be exactly six, and the corresponding eigenvector should represent six rigid body modes [41-43]. Both QUAD+ and TRIA+ shell element passed the zero energy mode test.

In order to pass the patch test, calculated stress fields should be constant [41-43]. Both QUAD+ and TRIA+ shell elements passed the patch tests.

3.2 Benchmark test for displacement validation

Table 2 shows all the benchmark tests performed in the present research to compare the displacement results. Numerical solutions were normalised with respect to the benchmark solutions. The following sub-sections describe the test cases with related results.

Table 2: Summary of benchmark tests for displacement validation used in the paper

Description		Test ID	Reference	Benchmark solution	Feature
Straight Cantilever Beam	Out-of-plane	1	Macneal and Harder [39] White and Abel [44]	w = -0.432	In-plane mesh distortion
	In-plane	2		v = -0.108	
	Twist	3		w = 3.208E-4	
Curved Cantilever Beam	In-plane	4		v = -0.08734	General locking
	Out-of-plane	5		w = -0.502	Shear Locking
Cook's skew beam		6	Stricklin, et al. [45] Bäcklund [28] Gifford [7] Lee and Bathe [46] Yuqiu and Yin [47] Piltner and Taylor [31] Cen, et al. [48]	v = 23.960	Membrane locking and mesh distortion
Scordelis-Lo Roof		7	Scordelis and Lo [49] Macneal and Harder [39] White and Abel [44]	v = 0.309	Complex membrane behaviour
Pinched Cylinder		8	Belytschko, et al. [50] White and Abel [44]	v = -1.825E-06	Membrane-bending coupling
Hemispherical Shell		9	Macneal and Harder [39] White and Abel [44]	w = 0.094	General locking in double-curved surface
Pre-twisted Cantilever Beam	In-plane	10	Musat and Epureanu [51] Gruttmann and Wagner [52]	w = -1.384	Out-of-plane mesh distortion (warping) Thickness = 0.05 (thin shell)
	Out-of-plane	11		v = 0.343	
	In-plane	12	Simo, et al. [53] Parisch [54] Sabourin and Brunet [55]	w = -5.420E-03	Out-of-plane mesh distortion (warping) Thickness = 0.32 (thick shell)
	Out-of-plane	13		v = 1.754E-03	

3.2.1 Straight cantilever beam (Test 1, 2, 3)

Although the straight cantilever beam (Figure 1) was a simple test, it showed all the main issues encountered in structural finite elements analysis of shells (bending, shear, and twist). Loads were applied at the two vertices of the free edge.

The analysed QUAD meshes (regular, trapezoidal, and parallelogram) are depicted in Figure 1. TRIA mesh was obtained by splitting the related QUAD element along the diagonal side (dotted line in Figure 1). To understand the sensitivity to mesh distortion, three different load conditions are adopted:

- The out-of-plane (F_1 load) condition caused the bending of the beam, and therefore, the results showed that the out-of-plane behaviour of the shells for different meshes.
- For the in-plane (F_2 load) condition, a unit load was directed along the transverse axis so that in plane bending and shear deformations aroused. This problem allowed to estimate the sensitivity to shear locking phenomenon and the effects of the distorted mesh.
- The twist (F_3 load) condition intended to evaluate how the distortion influenced the torsional behaviour of the cantilever beam. In particular, a twist couple was generated by two opposite forces applied at the vertices of the free edge.

Figures 2 to 4 report the normalised displacements for three different load conditions mentioned above. It was observed that QUAD elements performed very well both for regular meshes and distorted elements (parallelogram or trapezoidal).

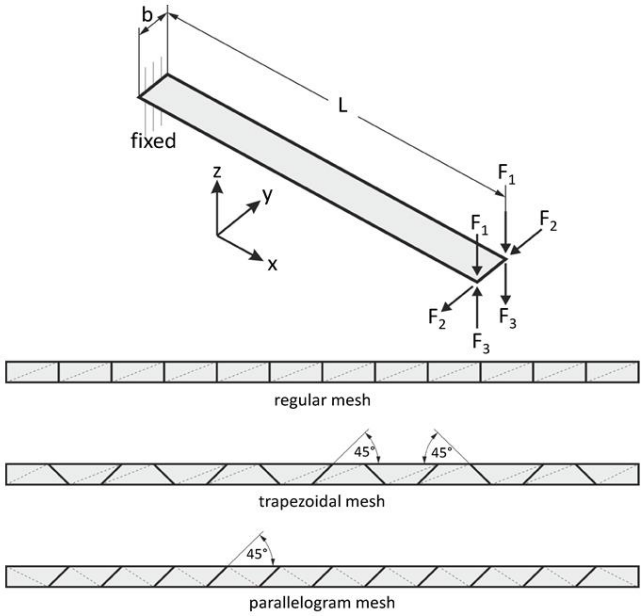

Figure 1 : Straight cantilever beam test (L=6.0; b=0.2; thickness=0.1; E=1.0E7; ν = 0.3; F1=F2=F3=0.5)

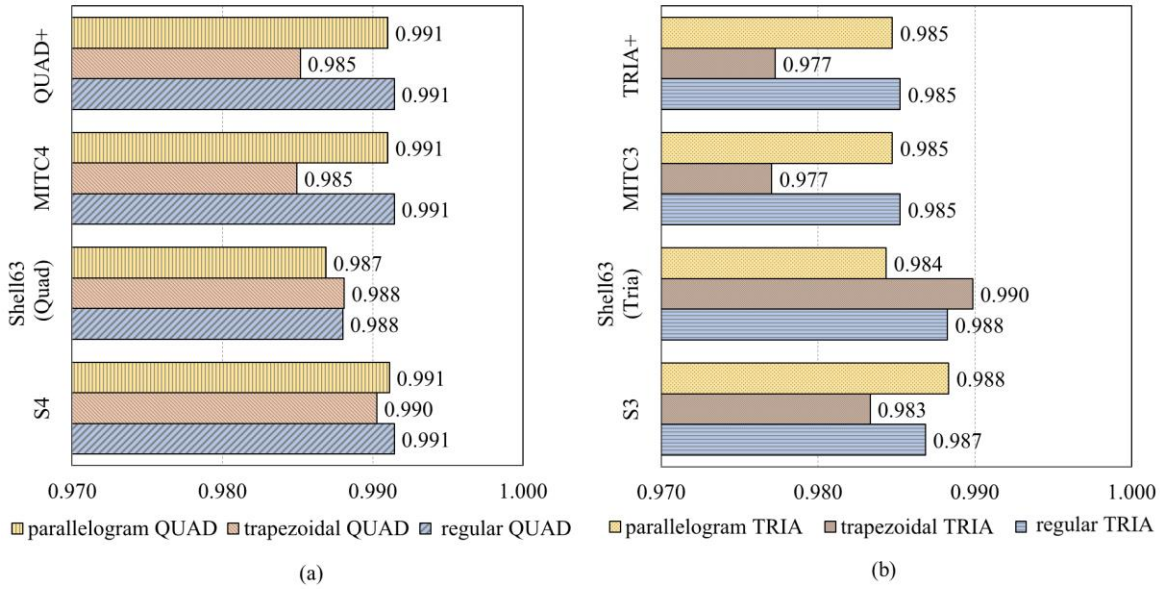

Figure 2: Results of out of plane condition for straight cantilever beam; (a) results for quad elements; (b) results for tria elements

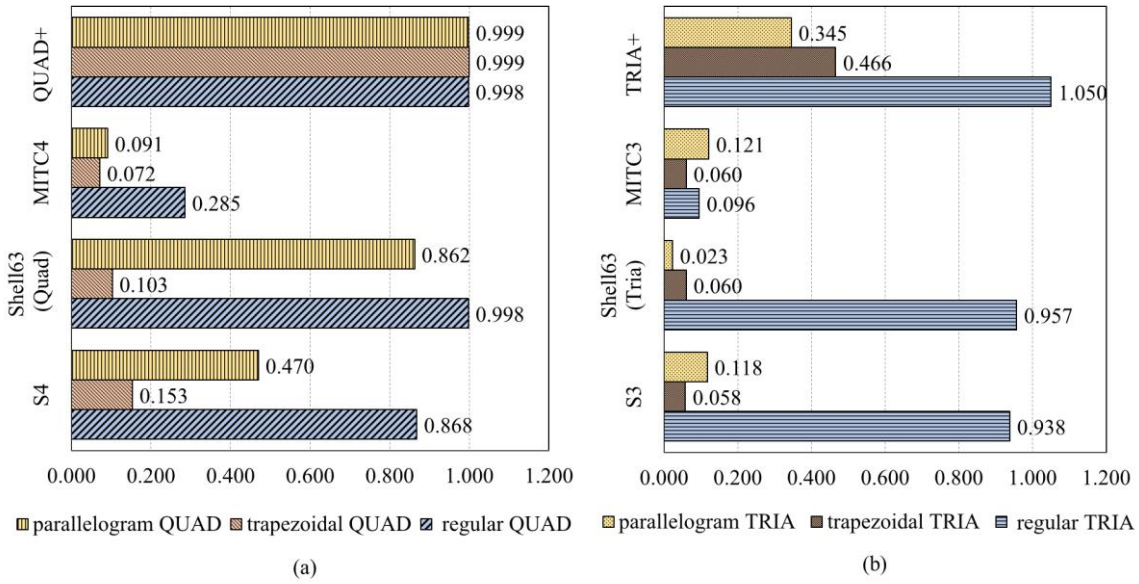

Figure 3: Results of in-plane condition for straight cantilever beam; (a) results for quad elements; (b) results for tria elements

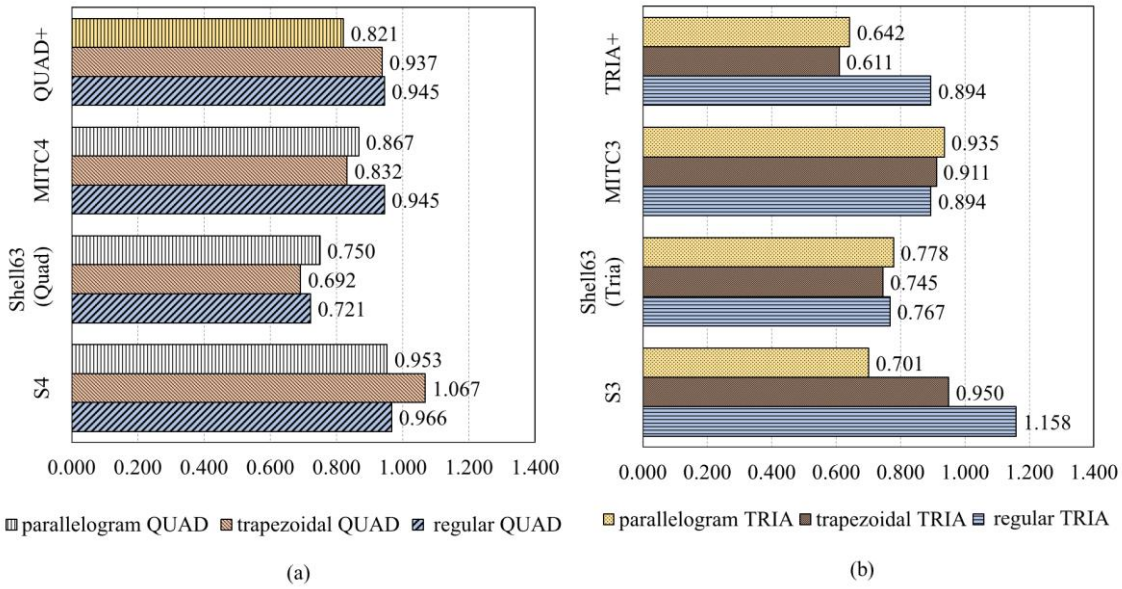

Figure 4: Results of twist condition for straight cantilever beam; (a) results for quad elements; (b) results for tria elements

However, MITC4 exhibited a poor behaviour for the in-plane load condition due to membrane/shear-locking. On the contrary, QUAD+ seemed to be quite insensitive to mesh distortion. Furthermore, as expected, TRIA elements were too stiff and the numerical solution converged slowly to the analytical reference value. On the contrary, TRIA+ and MITC3 elements appeared to be not reliable.

3.2.2 Curved Cantilever beam (Test 4, 5)

This test (Figure 5) involved membrane/shear locking and mesh distortion because a curved geometry was considered with in-plane (F_1 load) and out-of-plane (F_2 load) load conditions.

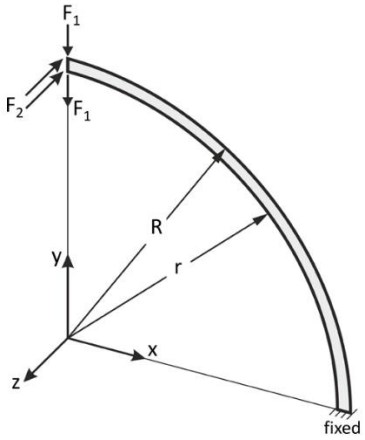

Figure 5: Curved cantilever beam test (R=4.32; r=4.12; thickness=0.1; E=1E7; ν = 0.25; F1=F2=0.5)

Simulations were carried out using different meshes to evaluate element convergence and efficiency. QUAD elements were gradually increased from 6 to 96 along the circumferential side, and from 1 to 4 in radial side, and thereafter, TRIA elements were obtained by splitting the related QUAD elements along the diagonal side. Displacements were calculated at free vertices in the direction of the load.

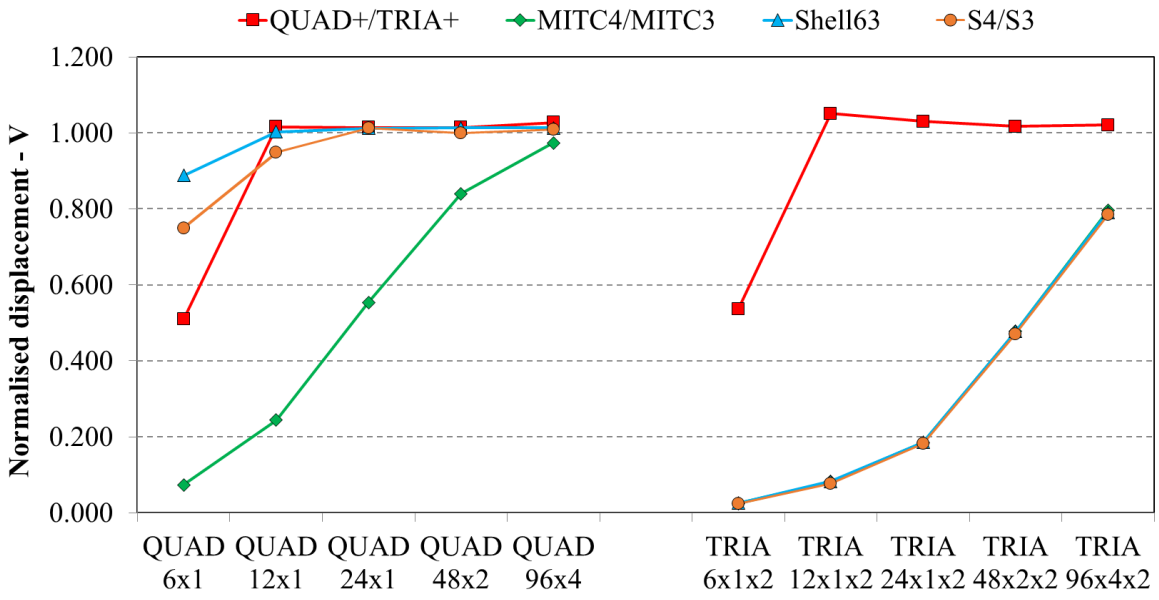

Figure 6: Curved cantilever beam results - in-plane load condition

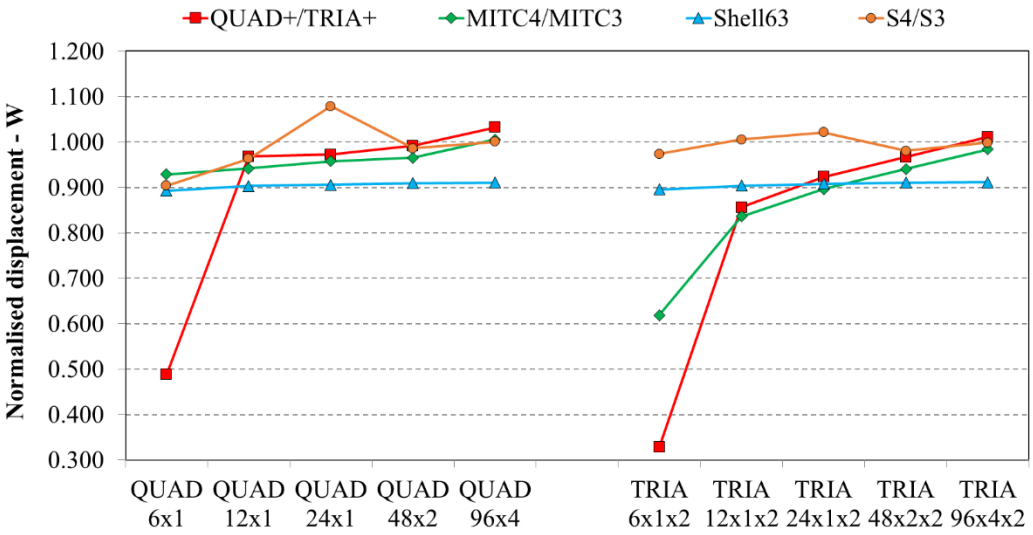

Figure 7: Curved cantilever beam results - out-of-plane load condition

Figures 6 and 7 depicts the normalised displacements for QUAD and TRIA elements varying the mesh density. With respect to the in-plane load condition, TRIA+ elements converged nicely to the reference solution whereas the others simulation packages failed to reach the satisfactory convergence. Moreover, the MITC4 exhibited the effect of the membrane locking when working in the in-plane load condition. Both for in-plane and out-of-plane conditions, QUAD+, S4 and Shell63 provided very efficient results since the convergence level was reached after just one refinement ("QUAD 12x1" in Figures 6 and 7).

3.2.3 Cook's skew beam (Test 6)

As shown in Figure 8, a skew cantilever beam is subjected to a shear load applied at the free edge.

Four different mesh refinements were tested as follows: elements were gradually increased from 2 to 16 on each side of the beam. Displacements were calculated at point P (Figure 8). Figure 9 represents the normalised displacements for QUAD and TRIA elements for varying the mesh size. The MITC4 slowly converged compared to other and QUAD+ performed superior to other. Similar results are observed for TRIA+.

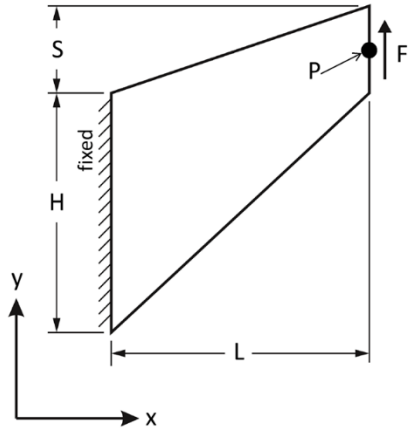

Figure 8: Cook's skew beam test (L=48.0; H=44.0; S=16.0; thickness=1.0; E=1.0; ν=1/3; F=1.0)

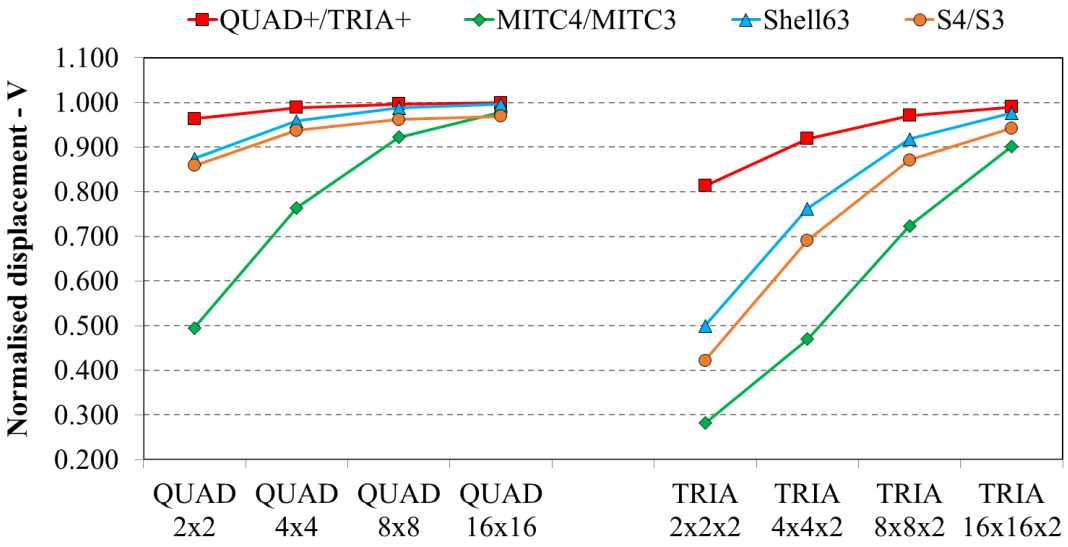

Figure 9: Cook's skew beam - normalised displacements of point "P"

3.2.4 Scordelis-lo roof (Test 7)

The test represented a barrel vault roof under self-weight (Figure 10). Complex states of membrane strain aroused in this test. Furthermore, the membrane locking phenomenon could not arise as the boundaries were not constrained along the z axis. Same number of elements was assigned on each side of the roof. The displacement along y axis of point "P" (Figure 10) was collected.

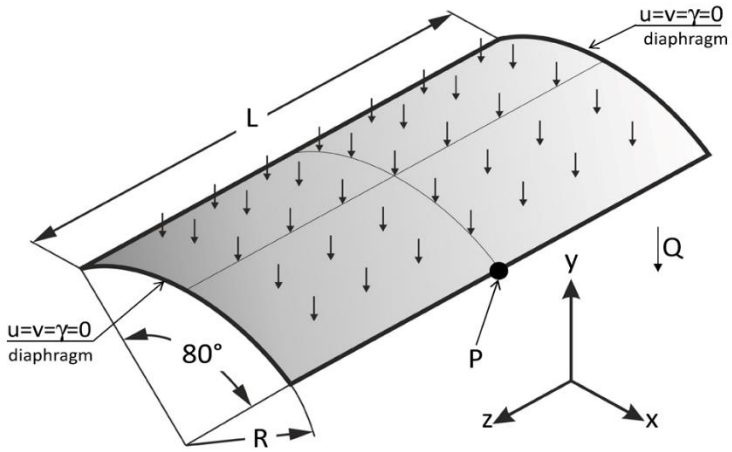

Figure 10: Scordelis-Lo roof test (R=25.0; L=50.0; thickness=0.25; E=4.28E8; ν = 0.0; Q=90.0)

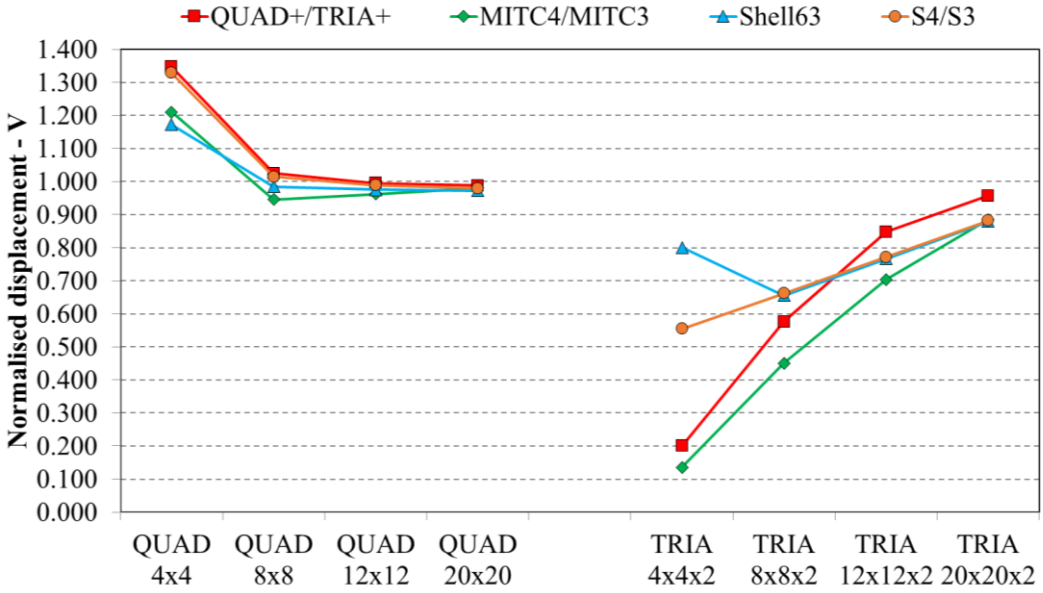

Figure 11: Scordelis-Lo Roof results - normalised displacements of point "P"

As shown in Figure 11, QUAD elements perform much better than the TRIA meshes. Moreover, when using QUAD elements, the membrane locking did not occur because the simulation converged to the normalised reference solution just after the first refinement of the mesh ("QUAD 8x8" in Figure 11).

3.2.5 Pinched cylinder (Test 8)

The pinched cylinder was one of the most severe tests to check the ability of elements to model both inextensional bending and complex membrane states (Figure 12). It was consisted of a cylinder with rigid end diaphragms (u=v=γ=0) and was loaded with two opposite forces, causing a bending-membrane coupling. Bending was just located in the areas close to the loading point, while membrane strains occurred far from the edges. Because of the symmetry of the problem, just one eighth of the cylinder was modelled using symmetry boundary constraints (same number of elements was assigned on each

side).

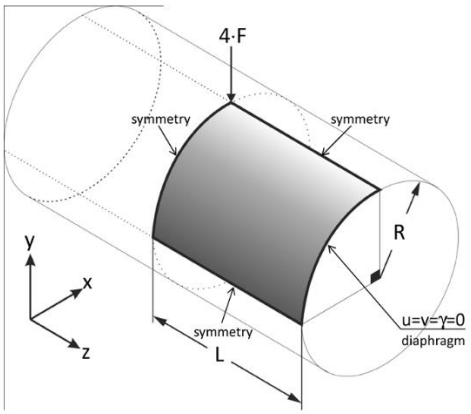

Figure 12: Pinched cylinder test (R=300.0; L=300.0; thickness=3.0; E=30.0E6; ν = 0.3; F=0.25)

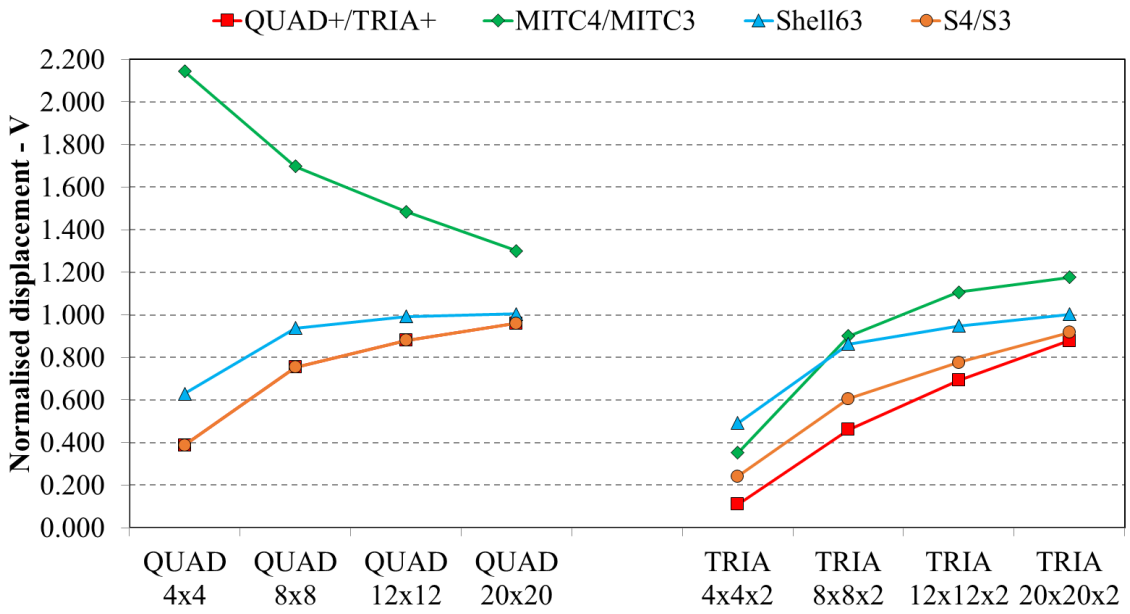

Figure 13: Pinched cylinder - results

Displacements were calculated at load point in direction of the force. Both MITC4 and MITC3 elements slowly converged to the reference solution (see Figure 13). On the contrary, Shell63 gave the best efficiency.

3.2.6 Hemispherical shell (Test 9)

This test dealt with a double-curved hemisphere shell (Figure 14). The hemisphere consisted of four point loads alternating in sign at 90° degree intervals on the equator. A hole with free edge was introduced at the top of the hemisphere to avoid triangular elements at the top. Only a quarter of the hemispherical shell structure was modelled and symmetrical boundary conditions were imposed on the side edges of the quarter hemisphere (same number of elements was assigned on each side). To avoid rigid displacement along the y axis, one point belonging to the equatorial plane was locked (v=0).

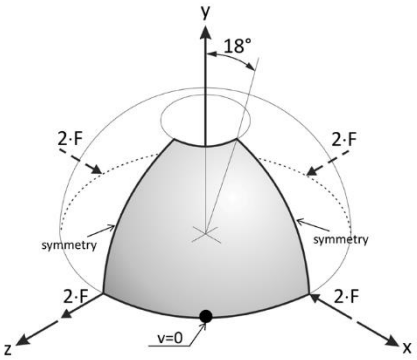

Figure 14: Hemispherical shell test (R=10.0; thickness=0.04; E=6.825E7; ν = 0.3; F=0.5)

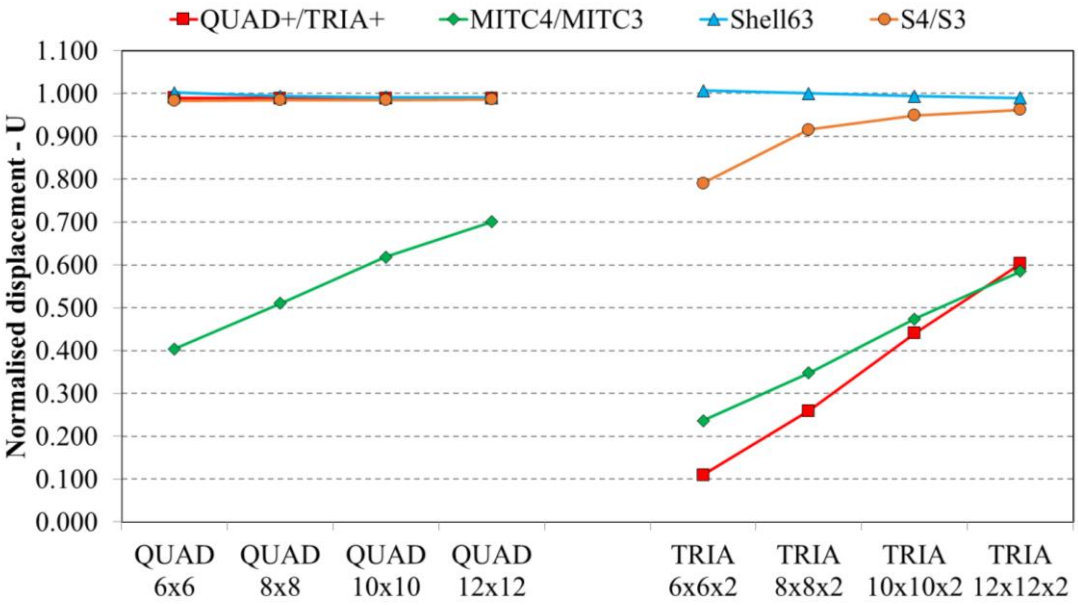

Figure 15: Hemispherical shell test - results

In this configuration, bending strains were predominant than membrane effects. As presented in Figure 15, results from QUAD+, Shell63 and S4 are satisfactory even with a very coarse QUAD mesh ("QUAD 6x6"). On the contrary, TRIA+ and MITC3 elements appeared not reliable and a mesh finer than 12x12x2 was required to get good results.

3.2.7 Pre-twisted beam (Test 10, 11, 12, 13)

The pre-twisted beam was obtained by sweeping a line along the beam axis while twisting it at a constant rate from 0 to 90° (see Figure 16). The beam was double-curved and the mesh was strongly affected by the warping effect, and thus, the bending-membrane coupling came into sight. Both in-plane (F_1 load) and out-of plane (F_2 load) load conditions were analysed.

Moreover, in order to highlight the sensitivity of the thickness, both thin (thickness=0.05) and thick (thickness=0.32) shells were analysed. Displacements were calculated at load point in direction of the force. QUAD elements were increased from 6 to 48 along the longitudinal axis and from 1 to 8 along the transversal axis.

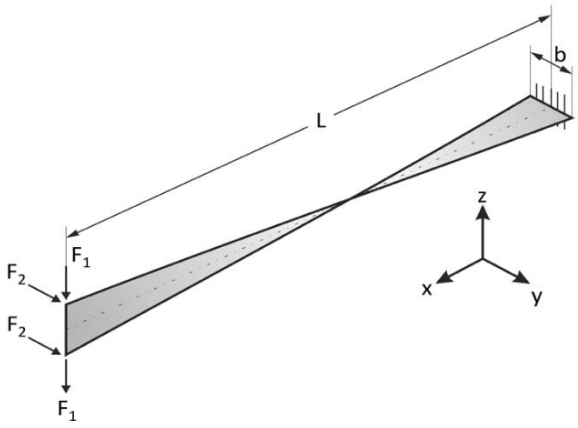

Figure 16: Pre-twisted beam test (L=12.0; b=1.1; E=29E6; ν = 0.22; F1=F2=0.5)

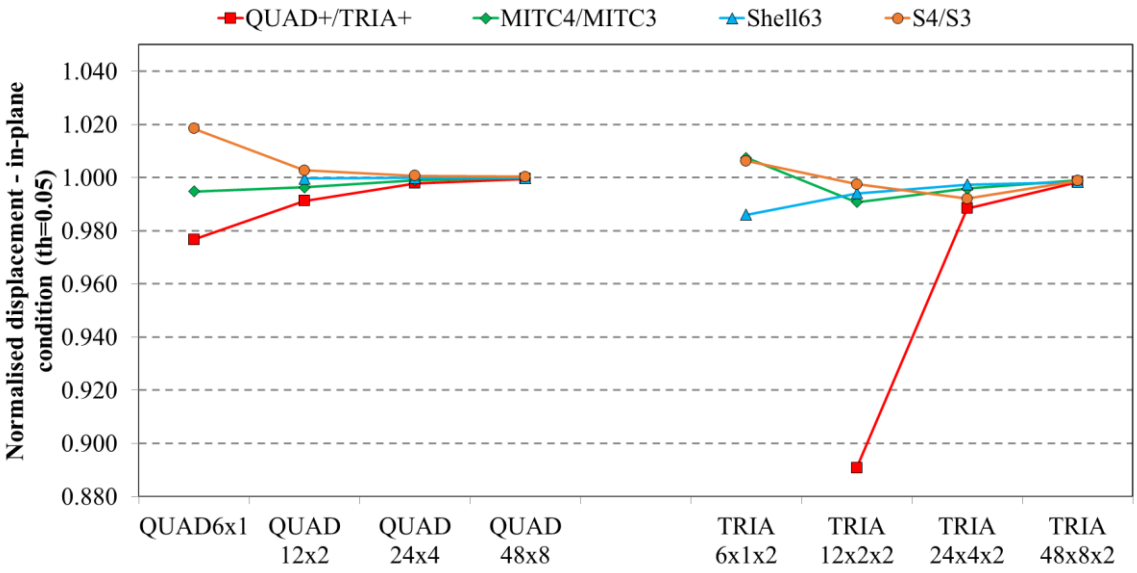

Figure 17: Pre-twisted beam results - in-plane condition (thickness=0.05)

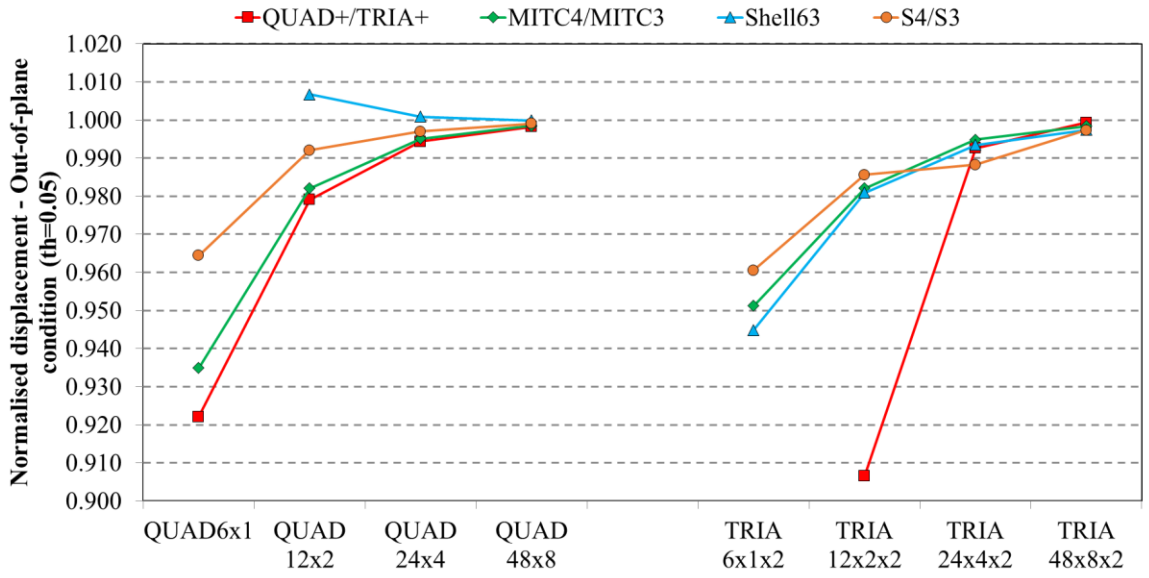

Figure 18: Pre-twisted beam results for out-of-plane condition (thickness=0.05)

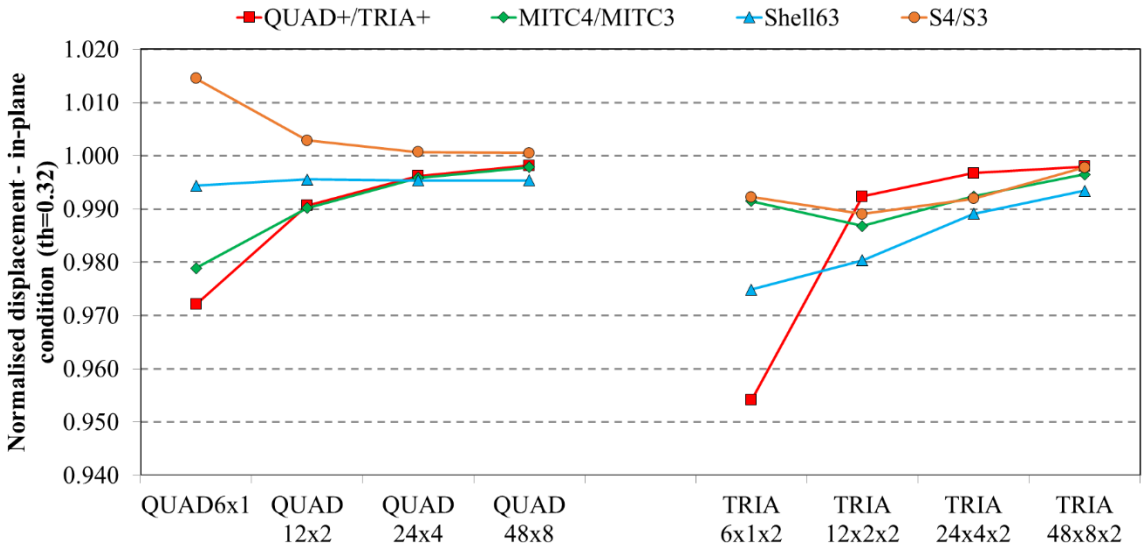

Figure 19: Pre-twisted beam results for in-plane condition (thickness=0.32 mm)

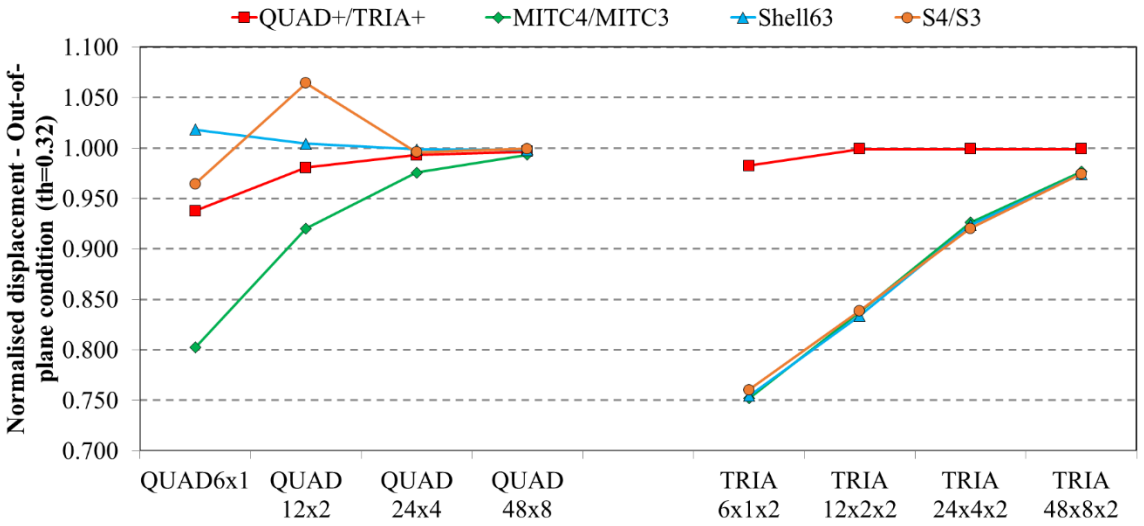

Figure 20: Pre-twisted beam results - out-of-plane condition (thickness=0.32 mm)

Figures 17 to 20 summarise the normalised displacement. For the thin structure (Figures 17 and 18), it was noticed that both TRIA+ and Sell63 (Quad) elements were completely failed (no result was obtained for those configurations) when working with a severe warping condition ("QUAD6x1" and "TRIA6x1x2", respectively). On the contrary, QUAD+ results were quite efficient for the thick shell configuration (Figure 19 and 20), showing a high convergence ratio even for the initial coarse mesh ("QUAD6x1" and "TRIA6x1x2", respectively).

3.3 Benchmark test for stress validation

Table 3 represents the tests used to validate the stress recovery. A brief overview of these test cases, along with the description of mesh construction is included in Appendix A. The QUAD+ and TRIA+ results were compared with benchmark values along with MITC4 and MITC3 results (Table 4).

Table 3: Summary of benchmark tests for stress validation used in the paper

Description	Test ID	Reference	Benchmark solution	Feature
Elliptic membrane	14	NAFEMs benchmark [40]	σ_{yy} = 92.7MPa	Membrane locking and mesh distortion
Cylindrical shell patch test	15		σ_{yy} = 60MPa	Warping effect
Z-section cantilever	16		σ_{xx} = -108MPa	General locking
Skew plate normal pressure	17		Max Principle stress = 0.802MPa	Mesh distortion
Thin shell beam wall in pure bending	18	Shigley and Mitchel [56]	Max bending stress = 2.16E4 PSI	Bending
Thin wall cylinder in pure tension	19	Roark and Young [57]	axial stress = 1E3 PSI	Membrane

Table 4: Results of the benchmark test for stress comparison with benchmark values

Description	Test ID	Element	Benchmark Solution	VRM	Error	COMSOL	Error
Elliptic membrane	14	Quad Coarse (3x2)	92.7MPa	80.33	-13.48%	73.01	-21.15%
		Quad fine (6x4)		88.42	-4.64%	88.38	-4.66%
		Tria Coarse (3x2x2)		71.44	-22.94%	49.68	-46.41%
		Tria fine (6x4x2)		78.82	-14.97%	70.63	-23.81%
Cylindrical shell patch test	15	Quad (θ=30°)	60MPa	51.80	-13.67%	82.12	36.87%
		Quad (θ=10°)		58.56	-2.40%	58.89	-1.85%
Z-section cantilever	16	Quad coarse (8x3)	-108MPa	-108.36	0.33%	-95.6	-11.45%
		Quad fine (40x15)		-107.69	0.33%	-115.12	6.59%
		Tria coarse (8x3x2)		-54.2	-49.81%	-94.18	-12.80%
		Tria fine(40x15x2)		-94.95	-12.08%	-115.45	6.90%
Skew plate normal pressure	17	Quad coarse (2x2)	0.802 MPa	0.3551	-55.73%	0.3551	-55.73%
		Quad fine (4x4)		0.7	-12.71%	0.70	-12.71%
		Quad fineer (20x20)		0.7819	-2.50%	0.7819	-2.50%
Thin shell beam wall in pure bending	18	Quad (50x10)	2.16E4 PSI	2.145E4	-0.69%	2.145E4	-0.69%
		Tria (50x10x2)		21.387E4	-0.98%	21.38E4	-.98%
Thin wall cylinder in pure tension	19	Quad (100x50)	1E3 PSI	1000.01	0.01%	999.67	-0.03%
		Tria (100x50x2)		1011.20	1.12%	991.10	-0.89%

Stress values, resulted from both QUAD+ and TRIA+ elements, were compared with benchmark values for each test cases except cylindrical shell patch test (test id 15). The original cylindrical shell patch test was defined for quad element and for θ=30° [40]. However, the test was carried out for θ=15° to reduce the warping effect as defined in [34]. TRIA elements were obtained by splitting the related QUAD elements along the one diagonal side. Therefore, in Table 4, the number of total TRIA elements is always double than the number of QUAD elements for the same test cases. It was observed that the stress calculation by QUAD+ and TRIA+ were comparable with the benchmark and also with MIC4/3 results as well.

4. Discussion

This paper uses a novel hybrid formulation (combination of two different formulations) to shell bending and membrane components for quadrilateral (QUAD+) and triangular element (TRIA+). This was implemented in Matlab so that it could be employed to simulate assembly operations involving sheet-metal parts along with other aspects such as robotic simulation, machine learning, variation modelling and many design areas where sheet metal parts can be employed. In order to reduce the computational time (in broader aspect - increase flexibility), which is somehow difficult when use Matlab alone (e.f. calculation of stiffness matrix), the computationally expensive functions/steps are converted into a Mex file using C++ coding, and then embedded into the Matlab script codes. Also, parallel computing using 'OpenMP', that is an Application Program Interface (API) that may be used to explicitly direct multi-threaded, shared memory parallelism, is used when feasible while developing Mex file.

There are many tests available in the literature for shell element testing, and the objective was to check how the mesh element works under bending and membrane dominant problem (or combination of both) to avoid membrane, shear locking effects along with mesh distortion effects. Therefore, the benchmark tests, which were mostly used as well as covered majority of the aspects of the shell element testing, were carefully selected. The pinched cylinder with a diaphragm is one of the most severe tests

for both inextensional bending modes and complex membrane states [44, 50], and it includes both the effect of performing 'clamped cylindrical shell' (membrane dominated problem) and 'free cylindrical shell' (bending dominated problem). In addition, it was mentioned that any element that passes the diaphragm support test problem will perform well when the boundary condition is simplified to a free boundary conditions [50]. Also, in recent paper by Prof. Bath and his group [5], the pinched cylinder with a diaphragm was included instead of free/clamped cylindrical test for MITC4+ formulation testing. Therefore, pinched cylinder with a diaphragm test was selected over by free/clamped cylindrical test. Moreover, complex states of membrane problem is examined through Scordelis-Lo roof problem [44, 50] whereas Hemispherical Shell test [44] checks an element's ability to represent inextensional bending modes with general locking effects.

In order to validate the implementation of the FEM, this paper presents a benchmark study on shell element formulation used in three commercial FEA software (ABAQUS, ANSYS and COMSOL) and one home-made Matlab based tool. The focus of the study was on linear shell elements under linear elastic static conditions with small deformation that are widely adopted to model and simulate sheet-metal part structures. A set of performance tests was identified through literature review to explore the effects of several factors (mainly geometry shape, thickness, loads, boundary conditions, mesh) affecting the shell accuracy. In addition, the sensitivity of numerical results on mesh distortion (in-plane and out-of-plane distortion) and on membrane and shear locking phenomena were also highlighted**.** Results from these tests cases were graded according to the grade rules in Table 5.

Table 5: Rules for grading element accuracy [17]

Grade	Rule for percentage error
A	error < 5%
B	5% ≤ error < 15%
C	15% ≤ error < 30%
D	30% ≤ error < 50%
E	error > 50%

In cases where multiple meshes were tested for a single benchmark test, the grade was defined from the results of the finest mesh.

The poor result obtained in several tests with very coarse mesh (mainly with triangular elements) is common to most of the tested software and it agrees with some limitations of the linear formulation behind both kinds of elements. In particular, it is known that especially for triangular elements, the linear formulation of shape functions in presence of bending effects produces a poor response and it can be improved by adopting higher order elements or finer mesh. In Di G.R. Liu this known issue pushed towards a meshfree solution in which numerical operations are not confined within the element, even considering triangular discretization of the computational domain[58]. It was also observed that there was some missing results (Fig 18, Shell63) of the analysis in correspondence of very coarse mesh (the first trial), and the commercial codes fail in this case. This means that a mesh of at least a number of FEM elements is required to correctly run the simulation. This is quite normal when dealing with linear triangular elements.

Table 6 and 7 summarises the displacement-based benchmark results for QUAD and TRIA element respectively. When more than one benchmark test contributes to the same comparison criteria, the average grade was calculated. For example, in Table 6 "Test 1", "Test 2", "Test 3" and "Test 6" contribute to quantify the effect of the in-plane mesh distortion. The over-all grade was obtained by

averaging amongst these four tests. The percentage error was calculated with respect to the reference solutions listed in Table 2.

As shown in Table 6, QUAD+ achieves grade A for all seven case, whereas grade A achieves by other packages as follows: S4 6 (1 grade B), Shell63 5 (2 grade B) and MITC4 achieves only 4 (2 grade C and 1 grade D). Comparing these results, it can be stated that QUAD+ shell element has the highest efficiency amongst the compared software packages. In fact, its percentage errors were rarely over 5%, even with very coarse meshes. In particular, "Test 1" and "Test 2" showed that the AGQ6 membrane formulation exhibits low sensitivity to in-plane mesh distortion compared to other software packages.

Table 6: Summary of displacement-based benchmark results - QUAD elements

QUAD ELEMENTS

Comparison Criteria	Test ID	Grade			
		S4	**Shell63**	**MITC4**	**QUAD+**
In-plane mesh distortion	1	A	A	A	A
	2	D	C	E	A
	3	A	C	B	B
	6	A	A	A	A
		B	B	C	A
Membrane and in-plane shear locking	4	A	A	A	A
Transverse shear locking	5	A	B	A	A
Complex membrane state	7	A	A	A	A
Membrane-bending coupling	8	A	A	D	A
General locking in double-curved surface	9	A	A	C	A
Out-of-plane mesh distortion (warping)	10	A	A	A	A
	11	A	A	A	A
	12	A	A	A	A
	13	A	A	A	A
		A	A	A	A

Shell63(quad) element worked fine and results were comparable to those of S3 in many test cases. A minor sensitivity to mesh distortion was observed in "Test 2" (in-plane straight cantilever beam) and "Test 3" (twist-couple straight cantilever beam).

MITC4 showed good results when bending and membrane states were not coupled. In particular, it failed in "Test 2" and did not provide satisfactory results for "Test 8" (pinched cylinder) and "Test 9" (hemispherical shell). It shows that the element formulation in COMSOL is not robust enough for complex and mixed stress states. This weakness might be attributed to the missed drilling degree of freedom (only five DoFs are used to formulate the shell model in COMSOL).

Table 7: Summary of displacement-based benchmark results - TRIA elements

TRIA ELEMENTS

Comparison Criteria	Test ID	Grade			
		S43	**Shell63**	**MITC3**	**TRIA+**
In-plane mesh distortion	1	A	A	A	A
	2	D	D	E	D
	3	C	C	B	C
	6	B	A	B	A
		C	B	C	B
Membrane and in-plane shear locking	4	C	C	C	A
Transverse shear locking	5	A	B	A	A
Complex membrane state	7	B	B	B	A
Membrane-bending coupling	8	B	A	C	B
General locking in double-curved surface	9	A	A	D	D
Out-of-plane mesh distortion (warping)	10	A	A	A	A

As shown in Table 7, grade A achieves by software packages as follows: S3 3 (2 grade B and 2 grade C), Shell63 (3 grade B and 1 grade C), MITC3 only 2 (1 grade B and 3 grade C and 1 grade D), and TRIA+ 4 (2 grade B and 1 grade D). Comparing these results, it can be stated that the performance of the TRIA+ element is better than other packages (except 'Test 9').

Table 8 and 9 show the summary of stress calculation benchmark results with grade. It was observed that the stress calculation by QUAD+ elements achieved grade A for all the test cases whereas TRIA+ elements were able to achieve grade A in two test cases out of 4. In addition, these stress values were comparable to the values achieved through MITC4/3 formulation.

Table 8: Summary of stress-based benchmark results - QUAD elements

QUAD ELEMENT

Comparison Criteria	Test ID	Grade	
		MITC4	**QUAD+**
Elliptic membrane	14	A	A
Cylindrical shell patch test	15	A	A
Z-section cantilever	16	B	A
Skew plate normal pressure	17	A	A
Thin shell beam wall in pure bending	18	A	A
Thin wall cylinder in pure tension	19	A	A

Table 9: Summary of stress-based benchmark results - TRIA elements

TRIA ELEMENT

Comparison Criteria	Test ID	Grade	
		MITC3	**TRIA+**
Elliptic membrane	14	C	B
Z-section cantilever	16	B	B
Thin shell beam wall in pure bending	18	A	A
Thin wall cylinder in pure tension	19	A	A

As expected, QUAD+ elements showed higher performance than TRIA+ elements. More specifically, TRIA elements exhibited low efficiency for plane geometries with distorted mesh. From the results, it is expected that the best efficiency can be reached only adopting dominant quadrilateral mesh elements when working on real geometry with complex shape. Triangular elements can exhibit a satisfactory accuracy, but they converge too slowly to the reference solution. Obviously, better performance might be obtained by adopting quadratic (or cubic) elements. However, it could lead to higher computational time, and therefore, the computational efficiency will be reduced drastically. This is especially true when these elements are employed in non-linear simulations involving, for example, contact pairs or non-linear boundary conditions.

As COMSOL follows MITC4 and MITC3 formulation, the flexibility of the newly developed hybrid formulation was compared with COMSOL results only. From Table 6, it is observed that QUAD+ lowest grade was B, and it was only for one test id whereas MITC4 got one B, two C, one D and one E grade. Therefore, even for finer mesh, QUAD+ performed better than MITC4. Similar observation can be drawn from Table 7 to conclude that TRIA+ performed better than MITC3. As can be observed from Figure 3 (Test Id 2), MITC4 and MITC3 performance were poor compared to QUAD+ and TRIA+ respectively, and therefore, it improves efficiency. For test id 4, QUAD+ and TRIA+ converged well with coarse mesh (QUAD 12x1 and TRIA 24x1x2 respectively) compared to MITC4 (QUAD 96x4) and MTC3 (TRIA 96x4x2) results with varying mesh density (Figure 6). Similar observation obtained from figure 9 of test id 6, where accurate results were obtained for QUAD+ formulation with coarse QUAD 4x4 whereas MITC4 produced accurate results with finer QUAD 16x16. Similarly, TRIA+ converged with coarser mesh of TRIA 8x8x2 whereas MITC3 converged with finer TRIA 16x16x2. For test 8, MITC4 performed very poorly whereas QUAD+ reached to convergence with only 8x8 mesh (Figure 13). For the same test, TRIA+ also converges faster than MITC3. Similar fast convergence was obtained for test 9 (figure 15). Based on that, it could be concluded that the proposed formulation efficiency is better than MITC4 and MITC3 in majority of the test cases.

The benchmark problems with test id 7, 8, 9 and 10 (Table 2) were common between this study and the paper by Ko, et al. [5] where a new MITC4+ and MITC3+ formulation were developed. It was observed that the proposed hybrid formulation for quadrilateral (QUAD+) elements performed better in terms of convergence for two cases (pinched cylinder – test id 8 and Hemispherical shell – test id 9) compared to MITC4+ when regular mesh was considered. For other two cases, both quad shell elements (QUAD+ and MITC4+) performed similarly. Therefore, it could be concluded that the proposed hybrid formulation has the potential to produce comparable performance, compared to the most advanced shell element formulation available in the literature. In future work, geometric non-linearity i.e. large deformation features will be incorporated and tested with benchmark studies mentioned in [59-61].

5. Conclusion

The paper focuses on FEM implementation of shell elements by developing a novel hybrid formulation for both quadrilateral and triangular elements. This new formulation was motivated by the need to develop flexible and efficient model to enable assembly process simulation of compliant sheet-metal parts. An open-source C++ code enhanced by the OpenMP interface for multiprocessing programming was implemented, and simulation tests and benchmarks were compiled and executed within Matlab using the MEX API interface.

A novel hybrid formulation was used for bending and membrane components of shell elements. QUAD+ element was formulated combining AGQ6 and MITC to model membrane and bending/shear component respectively. Similarly, TRIA+ element was formulated using ANDES for membrane and

MITC for bending/shear component. A set of benchmark tests were identified to explore the effect of several factors affecting the computational accuracy, such as: geometry shape, thickness, loads, boundary conditions, and mesh size. Extensive benchmark studies were accomplished to evaluate the performance of the proposed hybrid formulation and the shell formulations used in three commercial software - ABAQUS, ANSYS and COMSOL under static linear elastic condition with small strain assumption. Furthermore, sensitivity of numerical results on mesh distortion (in-plane and out-of-plane distortion) and on membrane and shear locking phenomena were highlighted. It was observed that there was a significant difference in terms of efficiency. In particular, whereas the three commercial software packages suffer when working with in-plane mesh distortion, the proposed hybrid formulation gives the most efficient results. This proves that the newly developed algorithms are robust enough with respect to mesh distortion. In addition, it was concluded that amongst three commercial FEM packages, the shell formulation in ABAQUS performs better than ANSYS and COMSOL for the benchmark test cases. It was also identified that the best efficiency can be reached only by adopting dominant quadrilateral mesh elements compared to the triangular elements when working on real geometry with complex shape.

The developed model and implementation not only improve the efficiency but also is capable of improving the flexibility of simulating assembly process with compliant parts. Future research will expand the proposed model to include on the broader spectrum multi-scale scenarios, such as robot kinematics and path planning optimisation, part variation, fixture optimisation, and classification of deviation patterns.

Acknowledgement:

Authors acknowledge the support of WMG Centre High Value Manufacturing Catapult (HVMC), APC UK project: Chamaeleon - New lightweight Materials and Processing Technologies for Common Lightweight Architecture of Electric and Hybrid Powertrain Systems, and the EPSRC UK project EP/K019368/1: Self-Resilient Reconfigurable Assembly Systems with In-process Quality Improvement.

References

[1] M. Perrella, S. Gerbino, and R. Citarella, "Chapter 8 - BEM in Biomechanics: Modeling Advances and Limitations," in *Numerical Methods and Advanced Simulation in Biomechanics and Biological Processes*, M. Cerrolaza, S. J. Shefelbine, and D. Garzón-Alvarado, Eds.: Academic Press, 2018, pp. 145-167.

[2] T. Belytschko, Y. Krongauz, D. Organ, M. Fleming, and P. Krysl, "Meshless methods: An overview and recent developments," *Computer Methods in Applied Mechanics and Engineering,* vol. 139, no. 1, pp. 3-47, 1996/12/15/ 1996.

[3] G. Papazafeiropoulos, M. Muñiz-Calvente, and E. Martínez-Pañeda, "Abaqus2Matlab: A suitable tool for finite element post-processing," *Advances in Engineering Software,* vol. 105, no. Supplement C, pp. 9-16, 2017/03/01/ 2017.

[4] K.-J. Bathe, *Finite element procedures in engineering analysis*. Prentice-Hal, Inc, Englewood Cliffs, New Jersey, 07632, 1982.

[5] Y. Ko, Y. Lee, P.-S. Lee, and K.-J. Bathe, "Performance of the MITC3+ and MITC4+ shell elements in widely-used benchmark problems," *Computers & Structures,* vol. 193, pp. 187-206, 2017/12/01/ 2017.

[6] D. Chapelle† and K. J. Bathe, "Fundamental considerations for the finite element analysis of shell structures," *Computers & Structures,* vol. 66, no. 1, pp. 19-36, 1998/01/01/ 1998.

[7] L. N. Gifford, "More on distorted isoparametric elements," *International Journal for Numerical Methods in Engineering,* vol. 14, no. 2, pp. 290-291, 1979.

[8] J. Robinson, "Some new distortion measures for quadrilaterals," *Finite Elements in Analysis and Design,* vol. 3, no. 3, pp. 183-197, 1987/10/01/ 1987.

[9] J. Robinson, "Quadrilateral and hexahedron shape parameters," *Finite Elements in Analysis and Design,* vol. 16, no. 1, pp. 43-52, 1994/04/01/ 1994.

[10] O. C. Zienkiewicz, R. L. Taylor, and J. Z. Zhu, "The Finite Element Method: its Basis and Fundamentals (Seventh Edition)." Oxford: Butterworth-Heinemann, 2013, pp. 1-20.

[11] X.-M. Chen, S. Cen, Y.-Q. Long, and Z.-H. Yao, "Membrane elements insensitive to distortion using the quadrilateral area coordinate method," *Computers & Structures,* vol. 82, no. 1, pp. 35-54, 2004/01/01/ 2004.

[12] K.-J. Bathe and E. N. Dvorkin, "A four-node plate bending element based on Mindlin/Reissner plate theory and a mixed interpolation," *International Journal for Numerical Methods in Engineering,* vol. 21, no. 2, pp. 367-383, 1985.

[13] Dominique Chapelle and K.-J. Bathe, *The Finite Element Analysis of Shells - Fundamentals* (Computational Fluid and Solid Mechanics). Springer-Verlag Berlin Heidelberg, 2011, pp. XV, 410.

[14] C. A. Felippa and C. Militello, "Membrane triangles with corner drilling freedoms—II. The ANDES element," *Finite Elements in Analysis and Design,* vol. 12, no. 3, pp. 189-201, 1992/12/01/ 1992.

[15] C. A. Felippa and S. Alexander, "Membrane triangles with corner drilling freedoms— III. Implementation and performance evaluation," *Finite Elements in Analysis and Design,* vol. 12, no. 3, pp. 203-239, 1992/12/01/ 1992.

[16] C. A. Felippa and C. Militello, "Construction of optimal 3-node plate bending triangles by templates," *Computational Mechanics,* journal article vol. 24, no. 1, pp. 1-13, July 01 1999.

[17] Y. Zhang, H. Zhou, J. Li, W. Feng, and D. Li, "A 3-node flat triangular shell element with corner drilling freedoms and transverse shear correction," *International Journal for Numerical Methods in Engineering,* vol. 86, no. 12, pp. 1413-1434, 2011.

[18] G. Gendron, "A review of four PC packages for FE structural analysis," *Finite Elements in Analysis and Design,* vol. 28, no. 2, pp. 105-114, 1997/12/15/ 1997.

[19] P. Roache, *Verification and Validation in Computational Science and Engineering*. Hermosa Publishers, Albuquerque, NM, 1998.

[20] P. Franciosa, S. Gerbino, and S. Patalano, "Advanced User-Interaction with GUIs in MatLAB®," in *Engineering Education and Research Using MATLAB*, D. A. Assi, Ed., 2011.

[21] S. E. Oh and J.-W. Hong, "Parallelization of a finite element Fortran code using OpenMP library," *Advances in Engineering Software,* vol. 104, pp. 28-37, 2017/02/01/ 2017.

[22] A. Laulusa, O. A. Bauchau, J. Y. Choi, V. B. C. Tan, and L. Li, "Evaluation of some shear deformable shell elements," *International Journal of Solids and Structures,* vol. 43, no. 17, pp. 5033-5054, 2006/08/01/ 2006.

[23] C.-K. Choi, T.-Y. Lee, and K.-Y. Chung, "Direct modification for non-conforming elements with drilling DOF," *International Journal for Numerical Methods in Engineering,* vol. 55, no. 12, pp. 1463-1476, 2002.

[24] R. A. S. Moreira and J. Dias Rodrigues, "A non-conforming plate facet-shell finite element with drilling stiffness," *Finite Elements in Analysis and Design,* vol. 47, no. 9, pp. 973-981, 2011/09/01/ 2011.

[25] K.-J. Bathe, A. Iosilevich, and D. Chapelle, "An evaluation of the MITC shell elements," *Computers & Structures,* vol. 75, no. 1, pp. 1-30, 2000/03/01/ 2000.

[26] K. Alvin, H. M. de la Fuente, B. Haugen, and C. A. Felippa, "Membrane triangles with corner drilling freedoms—I. The EFF element," *Finite Elements in Analysis and Design,* vol. 12, no. 3, pp. 163-187, 1992/12/01/ 1992.

[27] "COMSOL Multiphysics Reference Manual, version 5.3", www.comsol.com,"

[28] J. Bäcklund, "On isoparametric elements," *International Journal for Numerical Methods in Engineering,* vol. 12, no. 4, pp. 731-732, 1978.

[29] P.-G. Lee, "A three-node triangular plate bending element based on mindlin/reissner plate theory and mixed interpolation," *KSME International Journal,* journal article vol. 13, no. 1, pp. 50-62, January 01 1999.

[30] K. Wisniewski, "Finite Rotation Shells. Basic Equations and Finite Elements for Reissner Kinematics," 1 ed. (Lecture Notes on Numerical Methods in Engineering and Sciences, 2010.

[31] R. Piltner and R. L. Taylor, "A systematic construction of B-bar functions for linear and non-linear mixed-enhanced finite elements for plane elasticity problems," *International Journal for Numerical Methods in Engineering,* vol. 44, no. 5, pp. 615-639, 1999.

[32] B. P. Naganarayana and G. Prathap, "Force and moment corrections for the warped four-node quadrilateral plane shell element," *Computers & Structures,* vol. 33, no. 4, pp. 1107-1115, 1989/01/01/ 1989.

[33] J. Robinson, "A warped quadrilateral strain membrane element," *Computer Methods in Applied Mechanics and Engineering,* vol. 7, no. 3, pp. 359-367, 1976/03/01/ 1976.

[34] "Dassault Systèmes, Simulia Corp. ABAQUS version 2016 documentation. Provi- dence: Dassault Systèmes, Simulia Corp.; 2016.."

[35] " ANSYS® Academic Research Mechanical, Release 18.1, Help System, Coupled Field Analysis Guide, ANSYS, Inc.,"

[36] T. J. R. Hughes and W. K. Liu, "Nonlinear finite element analysis of shells: Part I. three-dimensional shells," *Computer Methods in Applied Mechanics and Engineering,* vol. 26, no. 3, pp. 331-362, 1981/06/01/ 1981.

[37] K. D. Kim, G. R. Lomboy, and G. Z. Voyiadjis, "A 4-node assumed strain quasi-conforming shell element with 6 degrees of freedom," *International Journal for Numerical Methods in Engineering,* vol. 58, no. 14, pp. 2177-2200, 2003.

[38] W. Kanok-nukulchai, "A simple and efficient finite element for general shell analysis," *International Journal for Numerical Methods in Engineering,* vol. 14, no. 2, pp. 179-200, 1979.

[39] R. H. Macneal and R. L. Harder, "A proposed standard set of problems to test finite element accuracy," *Finite Elements in Analysis and Design,* vol. 1, no. 1, pp. 3-20, 1985/04/01/ 1985.

[40] "NAFEMS Finite Element Methods & Standards, The Standard NAFEMS Benchmarks, Glasgow: NAFEMS, Rev. 3, 1990.."

[41] Y. Lee, P.-S. Lee, and K.-J. Bathe, "The MITC3+ shell element and its performance," *Computers & Structures,* vol. 138, pp. 12-23, 2014/07/01/ 2014.

[42] Y. Ko, P.-S. Lee, and K.-J. Bathe, "The MITC4+ shell element and its performance," *Computers & Structures,* vol. 169, pp. 57-68, 2016/06/01/ 2016.

[43] P.-S. Lee and K.-J. Bathe, "Development of MITC isotropic triangular shell finite elements," *Computers & Structures,* vol. 82, no. 11, pp. 945-962, 2004/05/01/ 2004.

[44] D. W. White and J. F. Abel, "Testing of shell finite element accuracy and robustness," *Finite Elements in Analysis and Design,* vol. 6, no. 2, pp. 129-151, 1989/12/01/ 1989.

[45] J. A. Stricklin, W. S. Ho, E. Q. Richardson, and W. E. Haisler, "On isoparametric vs linear strain triangular elements," *International Journal for Numerical Methods in Engineering,* vol. 11, no. 6, pp. 1041-1043, 1977.

[46] N.-S. Lee and K.-J. Bathe, "Effects of element distortions on the performance of isoparametric elements," *International Journal for Numerical Methods in Engineering,* vol. 36, no. 20, pp. 3553-3576, 1993.

[47] L. Yuqiu and X. Yin, "Generalized conforming triangular membrane element with vertex rigid rotational freedoms," *Finite Elements in Analysis and Design,* vol. 17, no. 4, pp. 259-271, 1994/11/01/ 1994.

[48] S. Cen, M.-J. Zhou, and X.-R. Fu, "A 4-node hybrid stress-function (HS-F) plane element with drilling degrees of freedom less sensitive to severe mesh distortions," *Computers & Structures,* vol. 89, no. 5, pp. 517-528, 2011/03/01/ 2011.

[49] A. C. Scordelis and K. S. Lo, "Computer Analysis of Cylindrical Shells," *Journal Proceedings,* vol. 61, no. 5, 5/1/1964 1964.

[50] T. Belytschko, H. Stolarski, W. K. Liu, N. Carpenter, and J. S. J. Ong, "Stress projection for membrane and shear locking in shell finite elements," *Computer Methods in Applied Mechanics and Engineering,* vol. 51, no. 1, pp. 221-258, 1985/09/01/ 1985.

[51] S. D. Musat and B. I. Epureanu, "Study of warping torsion of thin-walled beams with open cross-section using macro-elements," *International Journal for Numerical Methods in Engineering,* vol. 44, no. 6, pp. 853-868, 1999.

[52] F. Gruttmann and W. Wagner, "A linear quadrilateral shell element with fast stiffness computation," *Computer Methods in Applied Mechanics and Engineering,* vol. 194, no. 39, pp. 4279-4300, 2005/10/01/ 2005.

[53] J. C. Simo, D. D. Fox, and M. S. Rifai, "On a stress resultant geometrically exact shell model. Part II: The linear theory; Computational aspects," *Computer Methods in Applied Mechanics and Engineering,* vol. 73, no. 1, pp. 53-92, 1989/04/01/ 1989.

[54] H. Parisch, "An investigation of a finite rotation four node assumed strain shell element," *International Journal for Numerical Methods in Engineering,* vol. 31, no. 1, pp. 127-150, 1991.

[55] F. Sabourin and M. Brunet, "Analysis of plates and shells with a simplified three node triangular element," *Thin-Walled Structures,* vol. 21, no. 3, pp. 209-223, 1995/01/01/ 1995.

[56] J. Shigley and L. Mitchel, *Mechanical Engineering Design (4th Edition)*. New York: McGraw-Hill, Inc., 1983.

[57] R. Roark and W. Young, *Formulas for Stress and Strain*. New York: McGraw-Hill Book Company, 1989.

[58] L. G. R., *Meshfree Methods: Moving Beyond the Finite Element Method*, Second ed. CRC Press, 2009.

[59] T. J. R. Hughes and T. E. Tezduyar, "Finite Elements Based Upon Mindlin Plate Theory With Particular Reference to the Four-Node Bilinear Isoparametric Element," *Journal of Applied Mechanics,* vol. 48, no. 3, pp. 587-596, 1981.

[60] J.-L. Batoz and I. Katili, "On a simple triangular reissner/mindlin plate element based on incompatible modes and discrete constraints," *International Journal for Numerical Methods in Engineering,* vol. 35, no. 8, pp. 1603-1632, 1992.

[61] P. Boisse, J. L. Daniel, and J. C. Gelin, "A C0 three-node shell element for non-linear structural analysis," *International Journal for Numerical Methods in Engineering,* vol. 37, no. 14, pp. 2339-2364, 1994.